Cationic UV Curing of Bioderived Epoxy Furan-Based Coatings: Tailoring the Final Properties by in Situ Formation of Hybrid Network and Addition of Monofunctional Monomer

CATIONIC UV-CURING OF BIODERIVED EPOXY FURAN-BASED COATINGS. TAILORING THE FINAL PROPERTIES BY IN SITU FORMATION OF HYBRID NETWORK AND ADDITION MONOFUNCTIONAL MONOMER.

Lorenzo Pezzana†, Giuseppe Melilli‡, Nathanaël Guigo ‡, Nicolas Sbirrazzuoli‡ and Marco Sangermano†***

†: Dipartimento Scienza e Tecnologia dei Materiali, Politecnico di Torino, Corso Duca degli Abruzzi 24, Torino, 10100, Italy,

‡: Laboratory of Experimental Thermodynamics, UMR-CNRS-139, University of Nice-Sophia Antipolis, 06108 Nice 2, France

Corresponding authors: marco.sangermano@polito.it; Nicolas.Sbirrazzuoli@univ-cotedazur.fr

Lorenzo.pezzana@polito.it; giuseppe.melilli@unice.fr; Nathanael.GUIGO@univ-cotedazur.fr

KEYWORDS: 2,5-furandimethanol, epoxy, cationic UV-curing, biobased.

ABSTRACT

Biobased monomers are becoming essential to develop green products to substitute petroleum-based materials. In this study biobased monomers, such as furfuryl alcohol and 2,5-furandimethanol, are successfully functionalized with epoxy functional groups producing glycidyl furfuryl alcohol (GFA) and diglycidyl furfuryl alcohol (DGFA), respectively. Herein, DGFA is investigated as innovative cationic UV-curable monomer for coating applications. An easy tailoring of the properties of the final UV-cured coatings is demonstrated by varying the ratio of the DGFA:GFA or creating a hybrid coating by using tetraethyl orthosilicate (TEOS) as precursor of silica to form an inorganic network. Real-time Fourier Transform Infrared Spectroscopy (FT-IR) is used to monitor the cationic photopolymerization of DGFA formulations. Finally, glass transition, contact angle, thermal stability, and mechanical properties are investigated as function of TEOS and GFA content in DGFA formulations. The thermal mechanical behavior is studied by Dynamic Mechanical Thermal Analysis (DMTA). The thermal properties of the networks are analyzed by Dynamic Scanning Calorimetry (DSC) and Thermogravimetric Analysis (TGA).

1. INTRODUCTION

The concern about environmental climate change and the progressive depletion of petroleum feedstocks is leading toward the necessity to promote green alternative to petroleum-based materials currently employed in polymer synthesis [1]. The by-products of the food industry such as corn cobs, oat and rice hulls, sugar cane bagasse, cotton seeds, olive husks and stones, as well as wood chips has been estimated worldwide around 300,000 tons per year [2]. Thus, the large disposal of lignocellulosic biomass have caught a lot of attention as potential precursors of bio-based monomers to replace the fossil-based ones [2–4]. Furanic compounds, derived from carbohydrate biomass, are highlighted as promising substitutes of aromatic compounds that are totally dependent on petroleum reforming processes [5,6]. Examples of chemicals originated from two sugar units such as pentose (hemicellulose) and hexose (hemicellulose, cellulose) are reported in Figure 1. It is worth to note that a wide range of useful furanic-based substrates might be converted into a vast array of monomers and used in polymer synthesis. Thus, different applications can be targeted as such large portfolio of the biobased precursors opens the possibility to tailor the properties of the final materials [7,8].

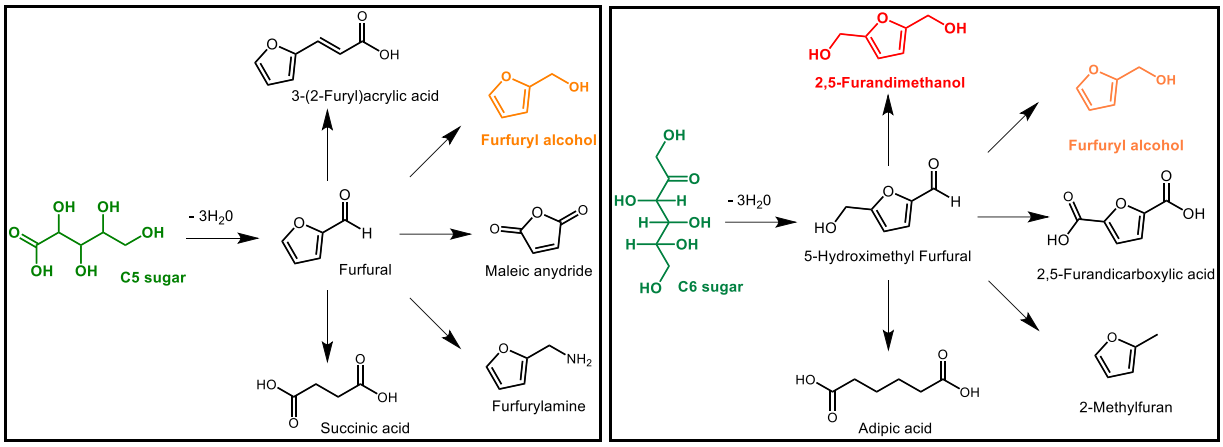

Figure 1. Example of monomers derived from furfural, pentose unit (left side) and 5-hydroxymethyl furfural, hexose unit (right side). The biobased monomers used as precursors in this paper are highlighted in red and orange.

Furfural and hydromethylfurfural are two interesting platforms chemicals. Furfural is derived from lignocellulosic biomass wastes such as agriculture and forestry residue [9,10]. The technology associated with furfural production is particularly simple, being based on the acid catalyzed hydrolytic depolymerization of the hemicellulose and the subsequent dehydration of the C5 glycosidic unit (Figure 1). C6 sugars can be also converted into hydroxymethylfurfural following a similar process [11–14].

Different monomers can be derived from these two units, for example 2-methylfuran has been used as biofuel [15], while 2,5-furandicarboxylic acid (FDCA) has found interesting applications in synthesis of biobased polyesters such as the spotlighted polyethylenefurandicaboxylate (PEF) bearing interesting mechanical, thermal and barrier properties [16–18]. Moreover FDCA has been studied for flame retardant properties as biobased epoxy coating [19].

Among all the available derivatives, the present study focalizes the research on furfuryl alcohol and 2,5-furandimethanol (Figure 1, orange and red chemical structures respectively) which have been already proposed in literature as bio-based polymeric precursors [20]. Furfuryl alcohol (FA) has been deeply studied due its unique possibility to self polycondense in polyfurfuryl alcohol (PFA) thermoset resins leading to the huge range of capabilities and fascinating properties in various fields of applications such as rocket fuels, foundry binders, wood modification and resin for aerospace and car industries [21,22]. 2,5-furandimethanol (FDM) has been proposed to produce coating with different properties by thermal curing [23], moreover it was used to develop an anticorrosive coating introducing TiO_2 as a filler [24].

The UV-curing technology has gained a lot of attention because considered as one of the most environmentally friendly process, solvent-free, and characterized by low energy consumption. These features resulted in energy and time saving, important characteristics for industrial processes [25,26]. The cationic UV-curing, introduced by Crivello [27–29], allowed to crosslink different precursors from epoxy to vinyl monomers. The mechanism involves the formation of cationic species by irradiating the formulation with UV-light. The initiation through onium salt occurs by the photoacid generation that starts the cationic chain growth polymerization process [26]. As previously mentioned, green resources are more and more used to produce new materials in order to limit the use of non-renewable resources [30,31], and this is becoming more and more important also for UV-curing process.

Epoxidized vegetables oils showed good reactivity in cationic photopolymerization with high possibility to tailor final properties of the crosslinked materials simply by modifying the stoichiometry of the formulation; in particular linseed oil and cardanol oil have been functionalized and used as starting monomers for coating applications [32,33]. Bio-renewable epoxy

monomers in cationic photopolymerization has been recently reported in a literature by Noè et al. [30]. In a previous work, the same authors showed an enhanced sustainable approach to the synthesis of epoxy functionalized bio-renewable monomers that can be applied in cationic photopolymerization [33–35]. Moreover, they reported the possibility to design the properties of the crosslinked materials by properly selecting the starting monomer.

To the best of our knowledge only few studies have been reported on the use of functionalized furan-based monomers for cationic photocurable applications. Cho et al. [36] reported the use of furanic compounds containing epoxy groups as alternatives to cationic photocurable petroleum-based adhesives.

In our study we developed an innovative UV-curable hybrid green coating based on epoxy functionalized FDM. In this context, we synthesized a diglycidyl furfuryl alcohol (DGFA) and a glycidyl furfuryl alcohol (GFA). The reactivity of the bifunctional epoxy monomer towards photoinduced cationic ring-opening polymerization was investigated.

With the aim of tailoring the final properties of DGFA coating we also investigated the influence of the addition of monofunctional epoxy monomer GFA and tetraethoxysilane (TEOS). In particular, a hybrid organic/inorganic network was produced, through a sol-gel process adding TEOS as precursor of the inorganic phase. The final properties of the UV-cured coatings DGFA/GFA and DGFA/TEOS were characterized and compared with the pristine DGFA.

2. MATERIAL AND METHODS

2.1.MATERIALS

2,5-furandimethanol, FDM (purity 97 %), was supplied by Apollo Scientific; furfuryl alcohol with purity of 98% (FA), epichlorohydrin (ECH) (purity > 99%), sodium hydroxide (NaOH),

tetrabutylammonium hydrogensulfate (TBHS), purity 97 %, magnesium sulphate ($MgSO_4$) were purchased by Sigma Aldrich. Tetrahydrofuran (THF), ethyl acetate, EtOAC, acetonitrile were supplied by Carlo Erba. NMR analysis was performed with chloroform, $CDCl_3$, provided by Sigma Aldrich. Tetraethyl orthosilicate (TEOS) and the photoinitiator, triarylsulfonium hexafluoroantimonate salts mixed to 50 wt% in propylene carbonate were purchased from Sigma Aldrich.

2.2.MONOMER SYNTHESIS

2.2.1. EPOXIDATION OF FURFURYL ALCOHOL

The synthesis of glycidyl furfuryl alcohol (GFA) was performed on the basis of previous protocol reported in literature [36,37]. The etherification reaction is reported in Scheme 1.

Epichlorohydrin (56.6 g, 0.61 mol) was poured into a three round bottom flask; a solution of NaOH 50 wt % (22.4 g, 0.56 mol) was added with the TBHS (0.66 g, 0.002 mol) was used as transfer catalyst. The solution was stirred for 30 min at room temperature, and nitrogen atmosphere was provided to the system. Furfuryl alcohol (20.0 g, 0.20 mol) was slowly added, and the reaction was left for 24 h at 50 °C. The reaction was stopped by adding ice water into the mixture. The product was extracted with ethyl acetate and dried over $MgSO_4$. The solvent was eliminated by vacuum distillation and the crude was left for 24 h in a vacuum oven (35 °C) to give yellowish liquid (25.0 g, yield 81 %). The ^1H NMR and ^{13}C NMR spectra give the following signals:

^1H NMR (400 MHz, CDCl3) δ 7.41 (t, J = 1.3 Hz, 1H), 6.34 (d, J = 1.6 Hz, 2H), 4.59 – 4.42 (m, 2H), 3.75 (dd, J = 11.5, 3.1 Hz, 1H), 3.44 (dd, J = 11.5, 5.8 Hz, 1H), 3.16 (ddt, J = 5.8, 4.2, 2.9 Hz, 1H), 2.79 (dd, J = 5.0, 4.1 Hz, 1H), 2.61 (dd, J = 5.0, 2.7 Hz, 1H).

^{13}C NMR (101 MHz, CDCl3) δ 151.39, 142.95, 110.31, 109.60, 70.59, 65.07, 50.74, 44.34.

Scheme 1. Epoxidation of furfuryl alcohol.

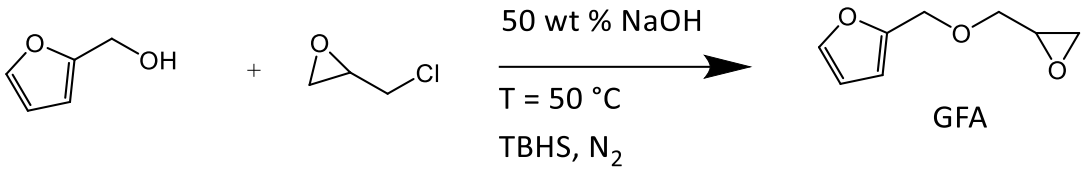

2.2.2. EPOXIDATION OF 2,5-FURANDIMETHANOL

The synthesis of diglycidyl furfuryl alcohol (DGFA) was carried out using a previous protocol reported in literature [23,36]. The etherification reaction is depicted in Scheme 2.

Epichlorhydrin (55.6 g, 0.60 mol) was poured into a three neck round bottom flask; solution of NaOH 50 wt % (20.6 g, 0.52 mol) was added with the TBHS (1.38 g, 0.004 mol) was used as transfer catalyst. The solution was stirred for 30 min at room temperature, meanwhile nitrogen atmosphere was provided to the system. FDM (5.5 g, 0.043 mol) was dissolved in THF (40 mL) and then added dropwise to the reaction. The reaction was left for 2 h at 50 °C. The reaction was stopped by adding ice water into the mixture. The product was extracted with ethyl acetate and dried over $MgSO_4$. The crude was purified by vacuum distillation and left in a vacuum oven (35 °C for 24 h) to give brownish viscous liquid (9.3 g, yield 90 %).

^{1}H NMR (400 MHz, CDCl3) δ 6.29 (s, 1H), 4.57 – 4.42 (m, 2H), 3.76 (dd, J = 11.5, 3.1 Hz, 1H), 3.44 (dd, J = 11.5, 5.8 Hz, 1H), 3.16 (ddt, J = 5.8, 4.1, 2.9 Hz, 1H), 2.79 (dd, J = 5.0, 4.1 Hz, 1H), 2.61 (dd, J = 5.0, 2.7 Hz, 1H).

^{13}C NMR (101 MHz, CDCl3) δ 151.94, 110.45, 70.85, 65.32, 50.86, 44.45.

Scheme 2. Epoxidation of FDM.

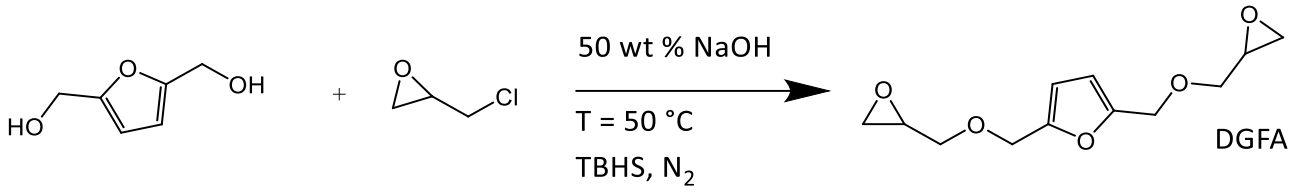

2.3. PHOTOPOLYMERIZATION

The different formulations were prepared as follows. The bifunctional monomer (usually around 0.4 g) was poured into a vial and then the photoinitiator was added as 2 parts per hundred resin (phr) (considering 100 parts the amount of monomer 2 parts of photoinitiator was addes). Then the vial was wrapped with aluminum foil to avoid light contact and the formulation was mixed mechanically for 5 min. The formulations were spread on glass substrate with a film bar ensuring a thickness of 150 μm. The photocuring was carried out by exposing the formulation to UV-light for 2 minutes. DMAX Flood lamp was used as UV-light source with light intensity set around 130 mW/cm^2. The emission spectrum of the UV-lamp was from 275 nm to 500 nm with a maximum located to 365 nm.

The formulations containing the monofunctional monomer were prepared in the same way modifying the weight ratio between the bifunctional and monofunctional monomer as described in Table 1. The photoinitiator was added in 2 phr with respect to the total amount of both monomers.

The formulations containing TEOS were prepared by mechanically mixing the silica precursor into the formulations. The addition was done in 30 and 50 phr with respect to the epoxy monomer. After 2 minutes of curing the films were treated at 150 °C for 4 hours in an oven providing high humidity atmosphere (by means of water bath inside the oven).

Table 1. Different formulations used in the study.

ENTRY	Formulation	DGFA/GFA (weight ratio)	TEOS (phr)	Photoinitiator (phr)
1	100 DGFA	100/0	-	2
2	90/10 DGFA/GFA	90/10	-	2
3	80/20 DGFA/GFA	80/20	-	2
4	70/30 DGFA/GFA	70/30	-	2
5	DGFA + 30 TEOS	100/0	30	2
6	DGFA + 50 TEOS	100/0	50	2

2.4.CHARACTERIZATION

2.4.1. NUCLEAR MAGNETIC RESONANCE (NMR)

NMR was conducted on a Bruker AM 400. ^{1}H-NMR and ^{13}C-NMR spectra were recorded at 400 MHz and 101 MHz respectively. $CDCl_3$ was used as solvent.

2.4.2. FOURIER TRANSFORM INFRARED SPECTROSCOPY (FT-IR)

A Nicolet iS 50 Spectrometer was used to record the data. All data were recorded as 32 scans with a spectral resolution of 4.0 cm^{-1} and handled with the software Omnic from Thermo Fischer Scientific. A silicon wafer was used as substrates for the transmission analysis. The liquid formulations were coated on the substrates with film bar guaranteeing a thickness of 32 µm. The conversion curves were collected by monitoring the disappearance of the epoxy peaks at 895 cm^{-1} and 857 cm^{-1}. The peak at 1550 cm^{-1} was taken as reference. It was assumed to be unaffected by UV-irradiation since it belonged to the C=C bending of the distributed furan [38]. Equation 1 was used to calculate the conversion during the exposure time [39–41].

$$Conversion = \frac{\left(\frac{A_{890}}{A_{1550}}\right)_{t=0} - \left(\frac{A_{890}}{A_{1550}}\right)_{t}}{\left(\frac{A_{890}}{A_{1550}}\right)_{t=0}} \quad \text{(Eq. 1)}$$

where A_{NN} is the area of the peak evaluated at different time and wavelength.

2.4.3. GEL CONTENT

The gel content percentage (% gel) of the photocured films was determined by measuring the weight loss after 24 h extraction with chloroform. The samples after the immersion were allowed to dry for 24 h in air. % gel was calculated according to Equation 2.

$$\%\ gel = \frac{W_1}{W_0} * 100 \quad \text{(Eq. 2)}$$

where W_1 is the weight of the dry film after the treatment with chloroform and W_0 is the weight of the dry sample before the treatment.

2.4.4. DYNAMIC MECHANICAL THERMAL ANALYSIS (DMTA)

The thermal mechanical analysis of the polymers was carried out with a Triton Technology instrument. The instrument applied uniaxial tensile stress at frequency of 1 Hz. The heating rate was 3 °C/min and the initial temperature of -20 °C was achieved by cooling down the test chamber with liquid nitrogen. The measurement was done to detect the T_g as maximum of tan δ curve and were stopped after the rubbery plateau. The tan δ represents the ratio between the loss modulus (E'') and the storage modulus (E'); the tan δ main peak is attributed to the cooperative motions during the alpha relaxation and thus its maximum can associated to the glass transition temperature, T_g [28]. The samples were UV-cured in a silicon mold with average dimension of 0.3 x 3.5 x 12 mm. Equation 3 is derived from the statistical theory of rubber elasticity and gives an estimation of the density of cross-links [42,43].

$$\nu_c = \frac{E\prime}{3RT} \quad \text{(Eq. 3)}$$

where ν_c is the number of crosslinks per volume of the crosslinked network, E' is the storage modulus in the rubbery plateau (i.e. T_g + 50 °C), R is the gas constant and T is the temperatureexpressed in Kelvin.

2.4.5. THERMOGRAVIMETRIC ANALYSIS (TGA)

The thermal stability of the coatings was studied by TGA by means of a Mettler Toledo TGA1. The selected method had a heating ramp of 10 °C/min from room temperature to 700 °C under N_2 atmosphere with flow of 40 mL/min. The analysis was done evaluating different features: T_5, temperature at which the sample lost 5 wt %; T_{peak}, temperature at peak of degradation, evaluated as peak of the first derivative and final char residue, analyzed as wt %.

2.4.6. DIFFERENTIAL SCANNING CALORIMETRY (DSC)

The DSC analysis was performed on a Mettler Toledo DSC-1 equipped with Gas Controller GC100. Samples of about 5-10 mg were sealed in 40 µl aluminum pans and analyzed by DSC. The data were analyzed with Mettler Toledo STARe software V9.2. The method used was the follow: the starting temperature was set as 30 °C; the first heating goes from 30 to 100 °C; then the temperature was maintained at 100 °C for 2 min in order to stabilize the sample, after that the chamber was again cooled until -20 °C was reached and then this temperature was maintained for 10 min, finally was a second heating from -20 °C to 300 °C applied. The first heating was done in order to eliminate the thermal history of the polymers. The heating and the cooling rates were set at 10 °C/min and the analysis was performed in a nitrogen atmosphere with a flow rate of 40 mL/min.

2.4.7. CONTACT ANGLE AND PENCIL HARDNESS

For the contact angle and pencil hardness tests, the films were beforehand photocured on glass substrate with a thickness of 150 μm. The contact angle test was performed with Drop Shape Analyzer, DSA100, Krüss. The water droplets were placed on free surface films and the results were an average value of at least 5 different droplets. The pencil hardness was measured according the standard ASTM D3363 [44]. For the hardness different pencils were used from 8 B to 8 H. The hardness value was defined as the last pencil (in order of hardness) that did not make a scratch on the film surface.

2.4.8. SCANNING ELECTRON MYCROSCOPY (SEM)

The microstructure of the hybrid material was investigated by scanning electron microscopy (JCM-6000PLUS, JEOL). The cross-section of the coating was realized by cryofracture. The coating was deep in liquid nitrogen for at least 5 minutes to ensure the cool down of the sample far below the glass transition. The surface of the fracture was coated with a Pt layer at a thickness of 5 nm. This inhibited charging, reduced thermal damage and improved the secondary electron signal required for the topographic examination.

3. RESULTS AND DISCUSSION

3.1.EPOXY MONOMERS SYNTHESIS

The biobased precursors, furfuryl alcohol and 2,5-furandimethanol, were used to synthesize epoxy functional monomers suitable for UV-curing applications. The synthesis was carried out in one step reaction with acceptable final yield and without side reactions as confirmed by NMR.

The final products, as confirmed by NMR analysis, were uncontaminated: no ECH or side product were detected. The synthesis shows two main advantages: (i) the relatively low reaction temperature, and (ii) fast reaction rate (around 90 % of yield in 4 h for DGFA). Furthermore, the purification steps did not require important amount of solvent and the ECH in excess can be easily removed in vacuum oven at 35 °C for 24 h avoiding critical further steps. Thus, the process could become suitable for large scale up. Figure 2 shows the ^{1}H-NMR spectra for the two synthetized monomers, the monofunctional epoxy (**GFA**) derived from furfuryl alcohol and the bifunctional (**DGFA**) derived from 2,5-furandimethanol.

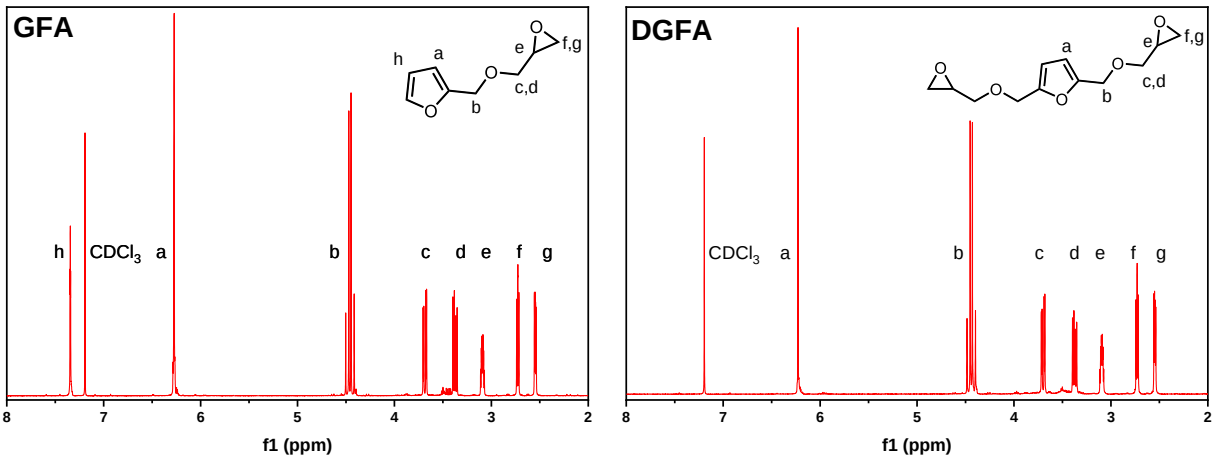

Figure 2. ^{1}H-NMR of the two synthesized monomers: **GFA**, left side, and **DGFA**, right side; $CDCl_3$ was used as solvent to conduct the analysis.

3.2.INVESTIGATION OF CATIONIC PHOTOPOLYMERIZATION

Cationic UV-curing process of DGFA/2 phr photoinitiator formulation was monitored by real-time FT-IR (Fig. 3). The first spectrum, collected without UV exposure (t = 0 sec), shows two peaks at 895 cm^{-1} and 857 cm^{-1} associated with the typical oxirane vibrations. Once the light turned on (t > 0 sec) these bands start to disappear as a consequence of the oxirane ring opening

[23,33,37]. The complete conversion was achieved after 120 s of irradiation at a light intensity irradiation of 130 W/cm^2. A broad peak in the region between 3,600 cm^{-1} and 3,200 cm^{-1} appeared simultaneously to the disappearance of the epoxy peaks. This indicated the formation of OH- groups due to the ring-opening polymerization reaction.

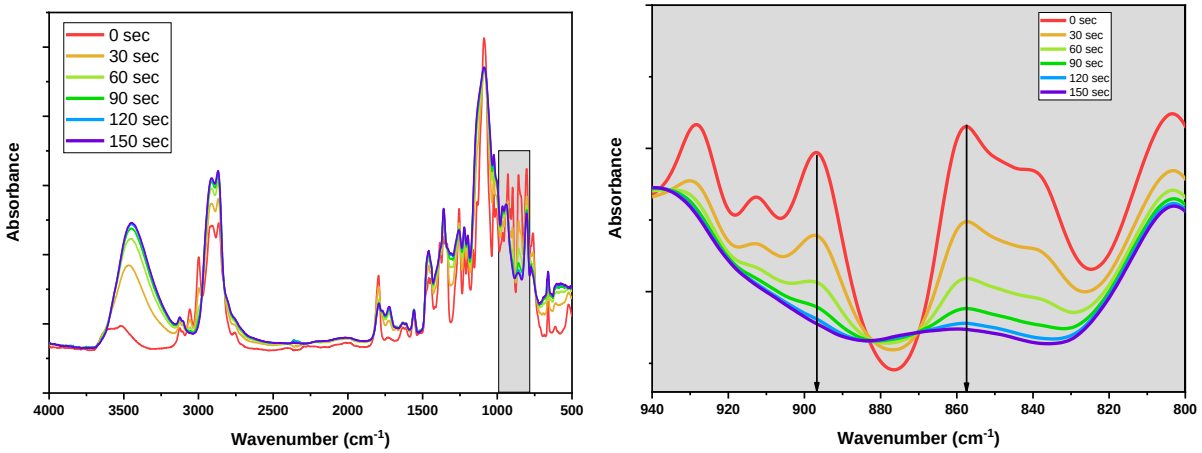

Figure 3. FTIR spectra of DGFA recorded during the UV-exposure (light intensity 130 W/cm^2). The formulation had a photoinitiator content of 2 phr. The expansion (yellow frame) shows the decrease of the characteristic peaks of epoxy ring situated in the region between 920 cm^{-1} and 830 cm^{-1}.

The first step in the cationic photocuring process was the evaluation of the most suitable photoinitiator content in the epoxy formulations. In Figure 4 the conversion curves as a function of irradiation time are reported for the cationic UV-curing of DGFA in the presence of 1,2 and 4 phr of cationic photoinitiator. The conversion was evaluated by the real-time spectra derived from FT-IR analysis. The calculation by means of Eq. 1 was done taking as a reference the band at 1,550 cm^{-1} which corresponds to the C=C bending of the distributed furan and remains constant all along the photocuring process because the UV-light does not affect the chemical

structure. An evident increase of the photocuring reactivity was reported doubling the photoinitiator content from 1 to 2 phr. After 30 s the conversion reached for the formulation containing 1 phr was around 30 % while using 2 phr of photoinitiator allowed to reach already 60 % of epoxy group conversion. The advantage of increasing the photoinitiator content up to 4 phr was limited in term of conversion and curing kinetics, so to maintain the lowest percentage possible of photoinitiator, 2 phr was used for all the different formulations. In this way the green content of the formulations was the highest possible preserving a rapid conversion in a limited amount of time.

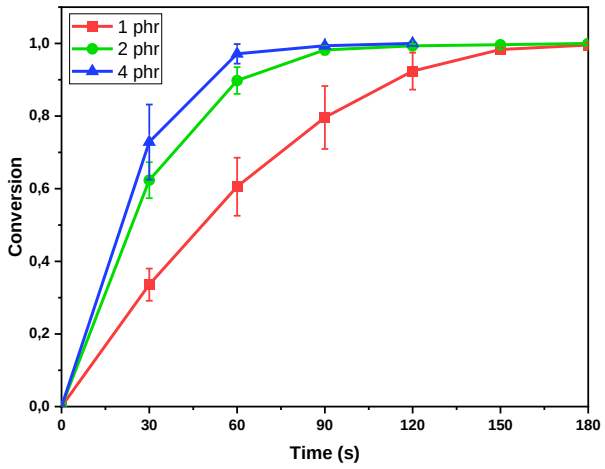

Figure 4. Conversion of epoxy group (from FT-IR) for the DGFA monomer as a function of the time changing the concentration of photoinitiator. The cationic photoinitiator was added in 1,2 and 4 phr. The light intensity was set as 130 W/cm^2.

3.3.THERMOMECHANICAL PROPERITES

Formulations based on DGFA were UV-cured with the aim to design coatings with different thermo-mechanical properties. Monofunctional epoxy monomer (10, 20, and 30 wt%) was added to DGFA to reduce the crosslinking density and tailor the final T_g of the cured coatings.

On the other hand, the rigidity of the UV-cured materials can be increased by dispersing in the organic matrix inorganic domains which can hinder the polymeric chain mobility with the enhancement of rigidity and the final T_g.

Hybrid material can be obtained by in situ sol-gel process, adding silica precursors such as TEOS into the formulation [45,46]. The process involves a series of hydrolysis and condensation reactions of hydrolysable multifunctional alkoxysilane [47,48]. Epoxy matrix has been used to form hybrid coatings. Sangermano et al. [49] developed a system based on nanosilica as filler obtaining enhancement of surface hardness and barrier properties. Linag et al. [50] shifted towards green monomers. Soybean oil and castor oil were used as epoxy functionalized starting monomers to generate the organic network. 3-glycidoxypropyl-trimethoxysilane was the precursor employed to form the inorganic network. The final coating had self-cleaning properties and improved thermal stability due to presence of inorganic counter part of network.

In Scheme 3 the representation of the two steps involved into this study for the formation of the hybrid material is depicted.

Scheme 3. Schematic representation of the two steps involves into the formation of the hybrid coating. Step 1: organic network formation by UV-curing; step 2: thermal treatment to produce the inorganic network.

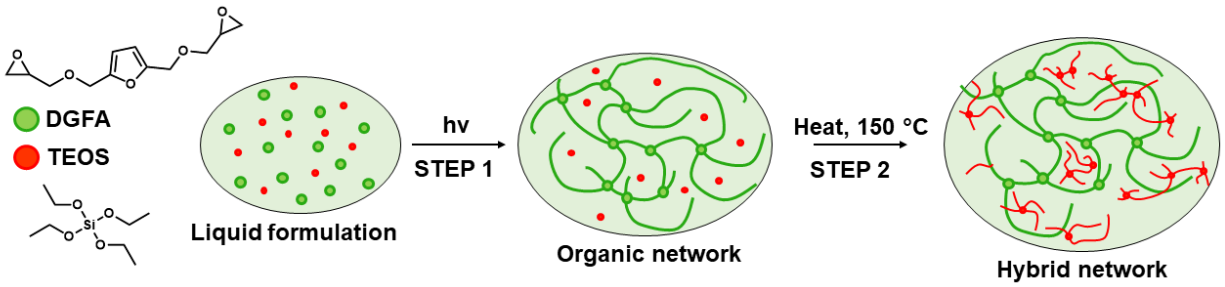

The UV-cured films were all fully crosslinked as evidenced by the very high gel content values evaluated for crosslinked samples (Table 2). Moreover, the curing kinetic and the final conversion of all different formulations were tested highlighting no influence neither by the introduction of the GFA or the TEOS as the conversion curves derived from real-time FTIR measurement confirmed (Figure S1).

The thermomechanical characterization was carried out by DMTA analyses. The DMTA analysis allows the screening of the viscoelastic properties of polymeric materials in a wide range of temperature. Figure 5 reports the tan δ curves from the DMTA analysis. It is possible to observe the influence of the monofunctional monomer into the formulations. The addition of the monomer GFA decreased the T_g due to the expected decrease of the crosslinking density as the consequence of the monofunctionality of GFA. The evaluation of cross-link density by means of Equation 3 confirmed that the addition of monofunctional monomer led to lower cross-linked network. The Table 2 summarizes all the data obtained from DMTA analysis. While the pristine DGFA crosslinked coating showed a T_g of 80 °C, a decrease of T_g values was measured for UV-

cured coatings obtained by DGFA formulations containing increasing content of GFA monomer. The coating obtained from the 70/30 DGFA/GFA formulation showed a T_g of 44 °C.

The broad shape of the tan δ peaks indicated crosslinked network heterogeneity and a wide distribution of chain segment mobility. A similar effect of monofunctional monomer was already reported in literature for a different UV-cured system [41].

T_g of UV-cured furan- and fatty acid-based thermosets were reported around 65 °C [32], which are slightly lower respect to the T_g of the pristine DGFA. Similar results have been also reported for thermal cured epoxy/anhydride system were T_g ranging from 29 to 70 °C [23]. Thus, considering this specific property, the UV-curing of the our DGFA formulation can compete with the thermal curing process leading to more sustainable one in term of energy requirement.

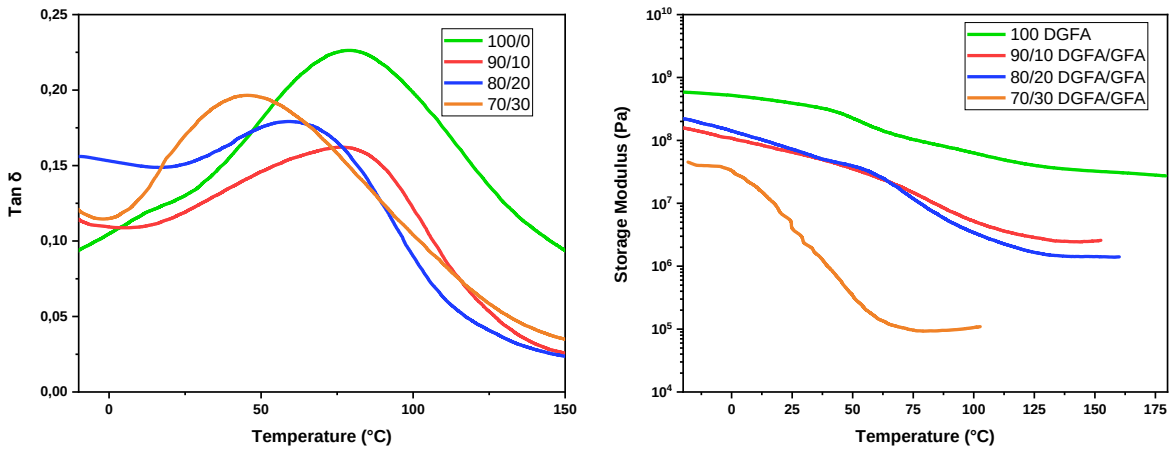

Figure 5. tan δ (left side) and storage modulus curves (right side) for the UV-cured coatings obtained by DGFA formulations containing increasing GFA monomer content.

The formulations DGFA/TEOS were fully cured after the UV-curing step. A thermal treatment of 150 °C in oven for 4 h was done on the UV-cured coating containing the precursor as reported in the experimental section. The silica can be formed in one step process at high temperature in

presence of acid catalyst and humid atmosphere, as demonstrated in previous studies [47,48]. In our study, the photoinitiator submitted to UV-irradiation guaranteed the presence of acid catalyst. The catalyst was crucial for the activation of the condensation process. Thus, after the formation of the organic polymeric matrix by UV-curing, the inorganic network was created by thermal treatment of the coatings (Scheme 3). After this treatment the samples were analyzed by DMTA. The Figure 6 showed the tan δ curves registered by DMTA analysis for the different investigated cured formulations. The tan δ peaks for the coatings obtained by the formulation containing 30 and 50 phr of TEOS shifted at higher temperature, when 30 phr of TEOS was added in the photolabile formulations only a limited enhancement of the T_g was achieved around 86 °C (i.e. + 6 °C compared to 100 DGFA), while the coating obtained from the formulation containing 50 phr of TEOS showed a T_g around 106 °C which correspond to a substantial increase (i.e. + 26 °C compared to 100 DGFA).

The addition of TEOS had also an important influence on the modulus in the rubbery region (Figure 6). In fact, the modulus of hybrid material was higher than the modulus of the pristine UV-cured DGFA. Moreover, considering the crosslink density it can be observed that it increased with the introduction of TEOS as consequence of formation of the hybrid network.

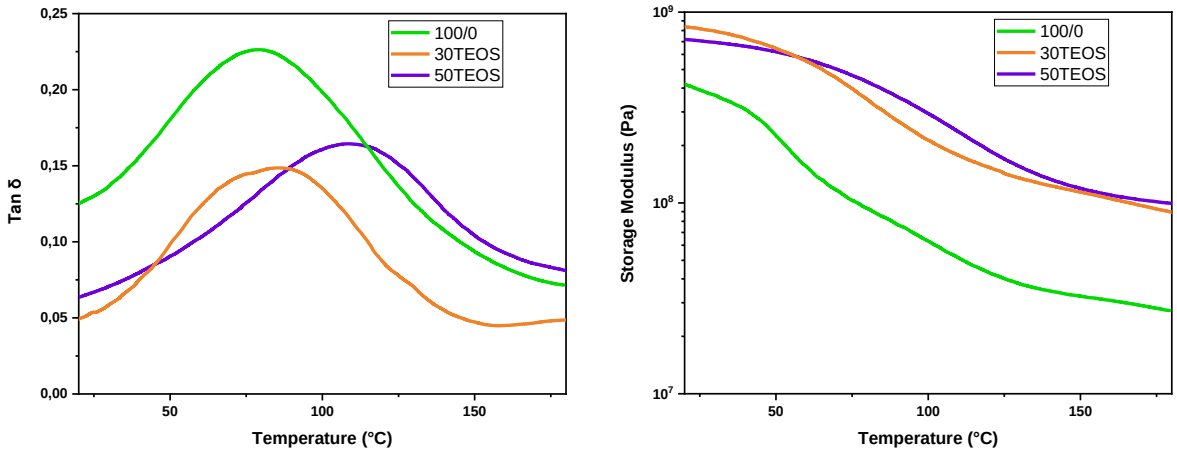

Figure 6. tan δ curves and storage modulus as a function of the temperature for the pristine DGFA network (100 DGFA) and for the hybrid materials with 30 phr TEOS (DGFA+30TEOS) and 50 phr of TEOS (DGFA+50TEOS).

Table 2. Results obtained for the different coatings obtained with the formulation described in section 2.3.

ENTRY	FORMULATION	T_g (1)	E (1)	ν_c (2)	% gel
		°C	MPa	mol/m^3	%
1	100 DGFA	80 ± 1	2.5 10^7 ± 0.5 10^7	7,465	94 ± 4
2	90/10 DGFA/GFA	75 ± 3	4.0 10^6 ± 0.2 10^6	1,194	93 ± 5
3	80/20 DGFA/GFA	59 ± 2	1.9 10^6 ± 0.1 10^6	598	90 ± 2
4	70/30 DGFA/GFA	44 ± 3	7.4 10^4 ± 0.5 10^4	24	91 ± 4
5	DGFA + 30TEOS	86 ± 4	1.1 10^8 ± 0.2 10^8	32,364	97 ± 3
6	DGFA + 50TEOS	106 ± 1	1.3 10^8 ± 0.1 10^8	36,465	96 ± 3

(1) evaluated by DMTA analysis and the maximum of the tan δ peak for the T_g

(2) calculated by Eq. 3

3.4.THERMAL PROPERTIES

The thermal properties of the polymeric coating were characterized by means of DSC and TGA. The results were reported in Table 3. The T_g trend observed by DMTA for the DGFA/TEOS and DGFA/GFA formulations were confirmed by DSC (Figure S2). In particular, the organic/inorganic network contributes to increase the T_g with respect to pristine DGFA. In contrast, the addition of the monofunctional GFA into the DGFA formulation results in a decrease of the T_g respect to the pristine DGFA (Table 3).

The T_g measurement by DSC was hard to achieve due to the slight variation of baseline in the thermograms. This result implying a high degree of heterogeneity of the cured network which was in accordance with the broad tan δ curves registered in DMTA.

The thermal stability of all crosslinked networks was studied by means of TGA. Figure 7 collects the curves for the cross-linked network obtained from the pristine DGFA UV-cured formulation (100 DGFA), from the film obtained in the presence of 30 wt% of monofunctional monomer (70/30 DGFA/GFA) and for the hybrid network obtained from the formulation containing 50 phr of TEOS (DGFA+50TEOS). We report only these three data since they had the most relevant results in terms of tailoring the final properties. The monofunctional monomer did not affected the thermal stability, indeed considering the T_5 and T_{peak} of the different networks, they were almost unaffected by the addition of GFA. This could be explained considering that the chemical structure of the two employed monomers was very similar, in both structures the pentose ring is the backbone of the molecules and both DGFA and GFA have the epoxy ring as functional group.

The weight lost of the UV cured formulations situated between 80 and 200°C could be explained by the reduced thermal stability of the non-reacted DGFA and GFA monomers. In

particular, T_5 of pure DGFA and GFA monomers occurred at relative low temperatures (180 °C and 110 °C respectively) with respect to the UV-cured formulations (Figure S3, S4). Furthermore, the presence of limited amount of unreacted monomers was proved by FTIR as well as % gel analysis enlightening the possibility to have a fraction of soluble part that can be released in the range of temperature between 80 °C and 200°C.

It is possible to see that the addition of TEOS lead to an increase of the thermal stability since the T_5 happened at higher temperature (i.e. almost + 60 °C) with respect to the network containing only the DGFA. Moreover, there was an increase of temperature at the peak of degradation (T_{peak}). The effect of the addition of TEOS is shown by the enhanced amount of the char at the end of the test which correspond to the additional silica residues. Thus, it can be stated that the creation of the hybrid network improved the thermal stability of the coating. This result was consistent with previous result reported in literature [47,48,50,51].

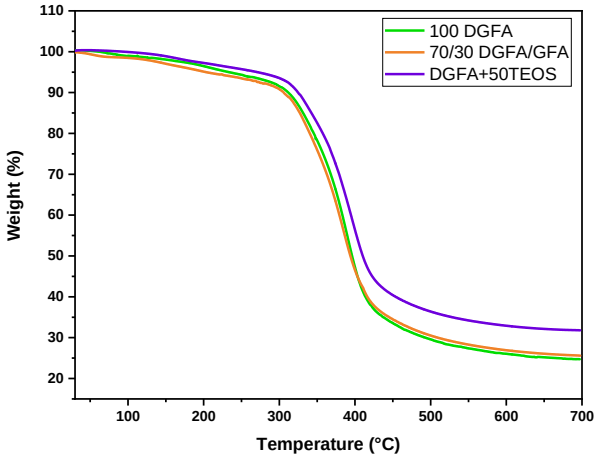

Figure 7. TGA curves of the pristine network (100 DGFA), network with 30 wt % of GFA (70/30 DGFA/GFA) and polymeric material with 50 phr of TEOS (DGFA+50TEOS).

Table 3. DSC and TGA results evaluated for the tested polymeric films.

ENTRY	FORMULATION	T_g (1)	T_g (2)	T_5 (3)	T_{peak} (3)	Char (3)
		°C	°C	°C	°C	%
1	100 DGFA	80 ± 1	83 ± 1	216 ± 4	380 ± 3	26
2	90/10 DGFA/GFA	75 ± 3	71 ± 3	213 ± 5	371 ± 3	24
3	80/20 DGFA/GFA	59 ± 2	61 ± 2	201 ± 5	389 ± 4	26
4	70/30 DGFA/GFA	44 ± 3	52 ± 4	205 ± 3	385 ± 2	25
5	DGFA + 30TEOS	86 ± 4	110 ± 2	231 ± 6	395 ± 5	30
6	DGFA + 50TEOS	106 ± 1	128 ± 3	274 ± 5	396 ± 2	32

(1) evaluated by DMTA analysis

(2) evaluated by DSC analysis

(3) evaluated by TGA

3.5.SURFACE PROPERTIES

The surface properties of the cured DGFA/GFA and DGFA/TEOS coatings were investigated by contact angle and pencil hardness tests. The contact angle of the UV-cured and thermally treated films decreased by introduction of TEOS in the photocurable formulations. This can be explained by the possibility to have additional OH group on the surface (derived from condensation reaction) that can reduce the hydrophobicity of the crosslinked network. In fact, the DGFA polymer had a contact angle of about 80°, (see Figure 8) while the coating obtained with 50 phr of TEOS showed a contact angle of 65°. The monofunctional monomer had no effect on the contact angle of the UV-cured coatings since the chemical structure of the GFA monomer was similar to the bifunctional DGFA.

Regarding the pencil hardness, as reported in the Table 4, the addition of TEOS increased the surface hardness of the coating as already reported in literature [47,49]. The in-situ formation of the inorganic domains homogeneously distributed within the polymeric matrix (see following SEM analysis), can importantly enhance the rigidity of the network, as observed by the increase of the T_g values, and therefore inducing an important increase on the surface hardness. On the other hand, the decrease of crosslinking density achieved in the presence of the monofunctional monomer did not affect the surface hardness of the crosslinked coatings.

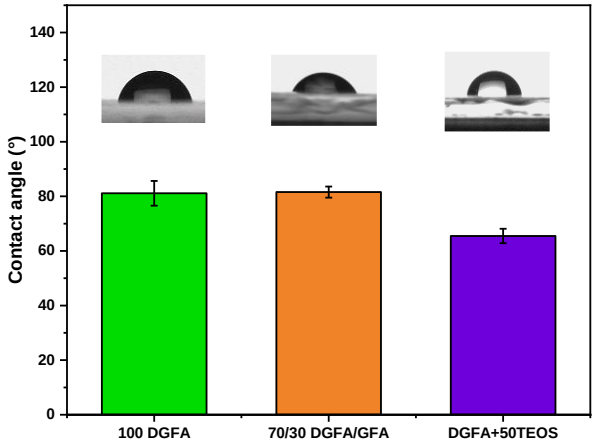

Figure 8. Contact angle evaluated for the cross-linked coatings. The results are the average value evaluated with at least 5 water droplets. Result for pristine DGFA, film with 30 wt % of FGA and film with 50 phr of TEOS are reported.

Table 4. Contact angle and pencil hardness results for the different coatings.

ENTRY	FORMULATION	Contact angle	Hardness
		°	
1	100 DGFA	81 ± 5	6H
2	90/10 DGFA/GFA	80 ± 2	5H
3	80/20 DGFA/GFA	83 ± 3	5H
4	70/30 DGFA/GFA	82 ± 2	5H
5	DGFA + 30TEOS	67 ± 3	8H
6	DGFA + 50TEOS	65 ± 3	8H

3.6.MORPHOLOGICAL ANALYSIS

In order to confirm the formation of the silica by means of the thermal treatment, SEM analysis were carried out on the cross-section surface of the DGFA/50TEOS coatings. The SEM images (Figure 9) confirms the presence of silica obtained by exposing the formed organic network to high temperature environment reach of humidity. The distribution of the spherical nanoparticles (average dimension 230 ± 50 nm) was quite homogeneous without important agglomerations.

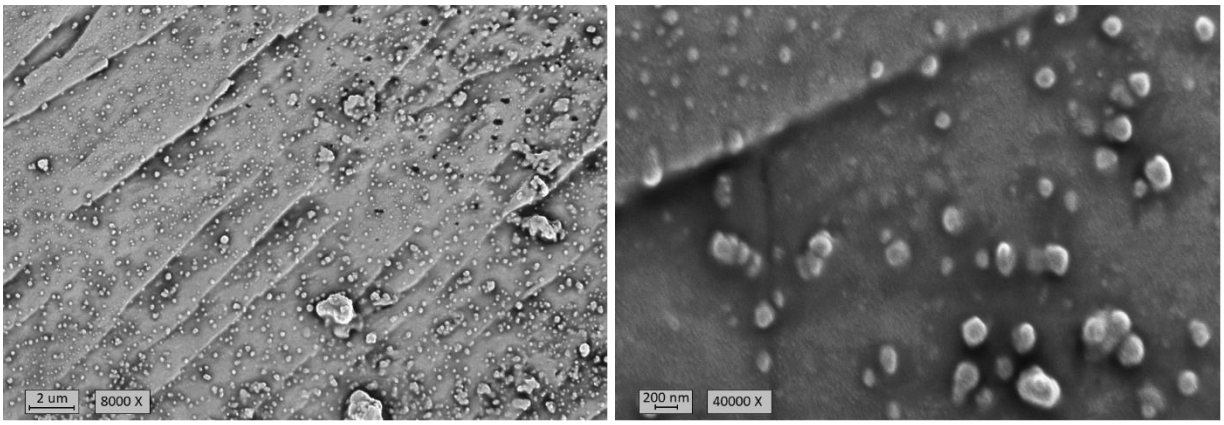

Figure 9. SEM images of coating containing 50 phr of TEOS. Magnification at 8,000 x and 4,000 x. The silica particles can be easily seen as white domains in the polymer organic matrix. From the imagine at 8,000 x the fragile fracture can be identified looking the fracture line present on the surface.

4. CONCLUSIONS

In this study, two bioderived furanic precursors, the furfuryl alcohol and the 2,5-furandimethanol were functionalized with epoxy groups. The synthesized monomers were used in cationic UV-curing process to obtain crosslinked coatings. With the aim of tailoring the final properties of the coating, the monofunctional glycidyl furfuryl alcohol (GFA) was added in different percentage, from 10 to 30 wt % content, in the DFGA monomer to modify the T_g of the crosslinked materials. As the FT-IR revealed, the monofunctional did not affect the conversion but had impacts on the thermomechanical properties. The second part of the study was the creation of hybrid organic-inorganic coatings to improve the properties of the pristine material obtained from DGFA. Therefore, TEOS was introduced as precursor to form an in-situ generated inorganic network via a sol-gel process. The formation of hybrid organic-inorganic coatings

occurred due to a post thermal treatment. The evaluation of the final properties revealed the effective improvement of modulus, T_g and hardness for hybrid materials. Moreover, the thermal stability was increased as confirmed by TGA analysis. Hence this study demonstrated the feasibility to achieve biobased UV-cured coating with the possibility to tailor the final properties according to the require target by simply modifying the starting photocurable formulations. A wide range of application can be fulfilled by the using of this system, considering the wide range of T_g from about 40 °C to 105 °C.

ASSOCIATED CONTENT

Supporting Information: DSC thermogram of all cured composites; TGA of pure GFA; TGA of pure DGFA.

AUTHOR INFORMATION

Corresponding Author

Nicolas Sbirrazzuoli: Nicolas.Sbirrazzuoli@univ-cotedazur.fr; Laboratory of Experimental Thermodynamics, UMR-CNRS-139, University of Nice-Sophia Antipolis, 06108 Nice 2, France

Marco Sangermano: marco.sangermano@polito.it; Dipartimento Scienza e Tecnologia dei Materiali, Politecnico di Torino, Corso Duca degli Abruzzi 24, Torino, 10100, Italy,

Author Contributions

The manuscript was written through contributions of all authors. All authors have given approval to the final version of the manuscript.

Funding Sources

Any funds used to support the research of the manuscript should be placed here (per journal style).

REFERENCES

(1) Bozell, J. J.; Petersen, G. R. Technology Development for the Production of Biobased Products from Biorefinery Carbohydrates—the US Department of Energy's "Top 10" Revisited. *Green Chem.* **2010**, *12* (4), 539–554. https://doi.org/10.1039/B922014C.

(2) Gandini, A. Monomers and Macromonomers from Renewable Resources. *Biocatalysis in Polymer Chemistry*. November 25, 2010, pp 1–33. https://doi.org/https://doi.org/10.1002/9783527632534.ch1.

(3) Zevallos Torres, L. A.; Lorenci Woiciechowski, A.; de Andrade Tanobe, V. O.; Karp, S. G.; Guimarães Lorenci, L. C.; Faulds, C.; Soccol, C. R. Lignin as a Potential Source of High-Added Value Compounds: A Review. *J. Clean. Prod.* **2020**, *263*. https://doi.org/10.1016/j.jclepro.2020.121499.

(4) Pezzana, L.; Malmström, E.; Johansson, M.; Sangermano, M. UV-Curable Bio-Based Polymers Derived from Industrial Pulp and Paper Processes. *Polymers* . 2021. https://doi.org/10.3390/polym13091530.

(5) Gandini, A.; Belgacem, M. N. Furans in Polymer Chemistry. *Prog. Polym. Sci.* **1997**, *22* (6), 1203–1379. https://doi.org/https://doi.org/10.1016/S0079-6700(97)00004-X.

(6) Belgacem, M. N.; Gandini, A. *Monomers, Polymers and Composites from Renewable Resources*; Elsevier, 2011.

(7) Gandini, A.; Belgacem, M. N. Chapter 6 - Furan Derivatives and Furan Chemistry at the Service of Macromolecular Materials; Belgacem, M. N., Gandini Polymers and Composites from Renewable Resources, A. B. T.-M., Eds.; Elsevier: Amsterdam, 2008; pp 115–152. https://doi.org/https://doi.org/10.1016/B978-0-08-045316-3.00006-5.

(8) Gandini, A.; Lacerda, T. M. From Monomers to Polymers from Renewable Resources: Recent Advances. *Prog. Polym. Sci.* **2015**, *48*, 1–39. https://doi.org/10.1016/j.progpolymsci.2014.11.002.

(9) Zeitsch, K. J. *The Chemistry and Technology of Furfural and Its Many By-Products*; Elsevier, 2000.

(10) Lee, Y.; Lee, J. Polymers Derived from Hemicellulosic Parts of Lignocellulosic Biomass. *Rev. Environ. Sci. Bio/Technology* **2019**, *18*, 317–334. https://doi.org/10.1007/s11157-019-09495-z.

(11) Román-Leshkov, Y.; Chheda, J. N.; Dumesic, J. A. Phase Modifiers Promote Efficient Production of Hydroxymethylfurfural from Fructose. *Science (80-.).* **2006**, *312* (5782), 1933–1937.

(12) Zhao, H.; Holladay, J. E.; Brown, H.; Zhang, Z. C. Metal Chlorides in Ionic Liquid Solvents Convert Sugars to 5-Hydroxymethylfurfural. *Science (80-.).* **2007**, *316* (5831), 1597–1600.

(13) Taarning, E.; Nielsen, I. S.; Egeblad, K.; Madsen, R.; Christensen, C. H. Chemicals from

Renewables: Aerobic Oxidation of Furfural and Hydroxymethylfurfural over Gold Catalysts. *ChemSusChem* **2008**, *1* (1–2), 75–78. https://doi.org/https://doi.org/10.1002/cssc.200700033.

(14) Iroegbu, A. O.; Sadiku, E. R.; Ray, S. S.; Hamam, Y. Sustainable Chemicals: A Brief Survey of the Furans. *Chem. Africa* **2020**, *3* (3), 481–496. https://doi.org/10.1007/s42250-020-00123-w.

(15) Tuan Hoang, A.; Viet Pham, V. 2-Methylfuran (MF) as a Potential Biofuel: A Thorough Review on the Production Pathway from Biomass, Combustion Progress, and Application in Engines. *Renew. Sustain. Energy Rev.* **2021**, *148*, 111265. https://doi.org/https://doi.org/10.1016/j.rser.2021.111265.

(16) Codou, A.; Guigo, N.; van Berkel, J.; de Jong, E.; Sbirrazzuoli, N. Non-Isothermal Crystallization Kinetics of Biobased Poly(Ethylene 2,5-Furandicarboxylate) Synthesized via the Direct Esterification Process. *Macromol. Chem. Phys.* **2014**, *215* (21), 2065–2074. https://doi.org/https://doi.org/10.1002/macp.201400316.

(17) de Jong, E.; Dam, M. A.; Sipos, L.; Gruter, G.-J. M. Furandicarboxylic Acid (FDCA), A Versatile Building Block for a Very Interesting Class of Polyesters. In *Biobased Monomers, Polymers, and Materials*; ACS Symposium Series; American Chemical Society, 2012; Vol. 1105, p 1. https://doi.org/doi:10.1021/bk-2012-1105.ch001.

(18) Codou, A.; Moncel, M.; van Berkel, J. G.; Guigo, N.; Sbirrazzuoli, N. Glass Transition Dynamics and Cooperativity Length of Poly(Ethylene 2,5-Furandicarboxylate) Compared to Poly(Ethylene Terephthalate). *Phys. Chem. Chem. Phys.* **2016**, *18* (25), 16647–16658. https://doi.org/10.1039/C6CP01227B.

(19) Meng, J.; Zeng, Y.; Chen, P.; Zhang, J.; Yao, C.; Fang, Z.; Guo, K. New Ultrastiff Bio-Furan Epoxy Networks with High Tg: Facile Synthesis to Excellent Properties. *Eur. Polym. J.* **2019**, *121*, 109292. https://doi.org/https://doi.org/10.1016/j.eurpolymj.2019.109292.

(20) Eid, N.; Ameduri, B.; Boutevin, B. Synthesis and Properties of Furan Derivatives for Epoxy Resins. *ACS Sustain. Chem. Eng.* **2021**, *9* (24), 8018–8031. https://doi.org/10.1021/acssuschemeng.0c09313.

(21) Iroegbu, A. O.; Hlangothi, S. P. Furfuryl Alcohol a Versatile, Eco-Sustainable Compound in Perspective. *Chem. Africa* **2019**, *2* (2), 223–239. https://doi.org/10.1007/s42250-018-00036-9.

(22) Guigo, N.; Mija, A.; Vincent, L.; Sbirrazzuoli, N. Eco-Friendly Composite Resins Based on Renewable Biomass Resources: Polyfurfuryl Alcohol/Lignin Thermosets. *Eur. Polym. J.* **2010**, *46* (5), 1016–1023. https://doi.org/https://doi.org/10.1016/j.eurpolymj.2010.02.010.

(23) Marotta, A.; Faggio, N.; Ambrogi, V.; Cerruti, P.; Gentile, G.; Mija, A. Curing Behavior and Properties of Sustainable Furan-Based Epoxy/Anhydride Resins. *Biomacromolecules* **2019**, *20* (10), 3831–3841. https://doi.org/10.1021/acs.biomac.9b00919.

(24) Marotta, A.; Faggio, N.; Ambrogi, V.; Mija, A.; Gentile, G.; Cerruti, P. Biobased Furan-Based Epoxy/TiO2 Nanocomposites for the Preparation of Coatings with Improved Chemical Resistance. *Chem. Eng. J.* **2021**, *406*, 127107. https://doi.org/https://doi.org/10.1016/j.cej.2020.127107.

(25) Scranton, A. B.; Bowman, C. N.; Peiffer, R. W. *Photopolymerization: Fundamentals and Applications*; ACS Publications, 1997.

(26) Sangermano, M.; Razza, N.; Crivello, J. V. Cationic UV-Curing: Technology and Applications. *Macromol. Mater. Eng.* **2014**, *299* (7), 775–793. https://doi.org/10.1002/mame.201300349.

(27) Crivello, J. V; Lam, J. H. W. Diaryliodonium Salts. A New Class of Photoinitiators for Cationic Polymerization. *Macromolecules* **1977**, *10* (6), 1307–1315. https://doi.org/10.1021/ma60060a028.

(28) Crivello, J. V; Narayan, R. Epoxidized Triglycerides as Renewable Monomers in Photoinitiated Cationic Polymerization. **1992**, No. 114, 692–699.

(29) Crivello, J. V; Liu, S. Photoinitiated Cationic Polymerization of Epoxy Alcohol Monomers. *J. Polym. Sci. Part A Polym. Chem.* **2000**, *38* (3), 389–401. https://doi.org/https://doi.org/10.1002/(SICI)1099-0518(20000201)38:3<389::AID-POLA1>3.0.CO;2-G.

(30) Noè, C.; Hakkarainen, M.; Sangermano, M. Cationic Uv-Curing of Epoxidized Biobased Resins. *Polymers (Basel).* **2021**, *13* (1), 1–16. https://doi.org/10.3390/polym13010089.

(31) Ng, F.; Couture, G.; Philippe, C.; Boutevin, B.; Caillol, S. Bio-Based Aromatic Epoxy Monomers for Thermoset Materials. *Molecules* . 2017. https://doi.org/10.3390/molecules22010149.

(32) Nameer, S.; Larsen, D. B.; Duus, J. O.; Daugaard, A. E.; Johansson, M. Biobased Cationically Polymerizable Epoxy Thermosets from Furan and Fatty Acid Derivatives.

ACS Sustain. Chem. Eng. **2018**, *6* (7), 9442–9450. https://doi.org/10.1021/acssuschemeng.8b01817.

(33) Noè, C.; Malburet, S.; Milani, E.; Bouvet-Marchand, A.; Graillot, A.; Sangermano, M. Cationic UV-Curing of Epoxidized Cardanol Derivatives. *Polym. Int.* **2020**, *69* (8), 668–674. https://doi.org/https://doi.org/10.1002/pi.6031.

(34) Noè, C.; Malburet, S.; Bouvet-Marchand, A.; Graillot, A.; Loubat, C.; Sangermano, M. Cationic Photopolymerization of Bio-Renewable Epoxidized Monomers. *Prog. Org. Coatings* **2019**, *133*, 131–138. https://doi.org/https://doi.org/10.1016/j.porgcoat.2019.03.054.

(35) Malburet, S.; Di Mauro, C.; Noè, C.; Mija, A.; Sangermano, M.; Graillot, A. Sustainable Access to Fully Biobased Epoxidized Vegetable Oil Thermoset Materials Prepared by Thermal or UV-Cationic Processes. *RSC Adv.* **2020**, *10* (68), 41954–41966. https://doi.org/10.1039/D0RA07682A.

(36) Cho, J. K.; Lee, J.-S.; Jeong, J.; Kim, B.; Kim, B.; Kim, S.; Shin, S.; Kim, H.-J.; Lee, S.-H. Synthesis of Carbohydrate Biomass-Based Furanic Compounds Bearing Epoxide End Group(s) and Evaluation of Their Feasibility as Adhesives. *J. Adhes. Sci. Technol.* **2013**, *27* (18–19), 2127–2138. https://doi.org/10.1080/01694243.2012.697700.

(37) Ye, J.; Ma, S.; Wang, B.; Chen, Q.; Huang, K.; Xu, X.; Li, Q.; Wang, S.; Lu, N.; Zhu, J. High-Performance Bio-Based Epoxies from Ferulic Acid and Furfuryl Alcohol: Synthesis and Properties. *Green Chem.* **2021**, *23* (4), 1772–1781. https://doi.org/10.1039/D0GC03946B.

(38) Guigo, N.; Mija, A.; Vincent, L.; Sbirrazzuoli, N. Chemorheological Analysis and Model-Free Kinetics of Acid Catalysed Furfuryl Alcohol Polymerization. *Phys. Chem. Chem. Phys.* **2007**, *9* (39), 5359–5366. https://doi.org/10.1039/b707950h.

(39) Jafarzadeh, S.; Johansson, M.; Sundell, P.-E.; Claudino, M.; Pan, J.; Claesson, P. M. UV-Curable Acrylate-Based Nanocomposites: Effect of Polyaniline Additives on the Curing Performance. *Polym. Adv. Technol.* **2013**, *24* (7), 668–678. https://doi.org/https://doi.org/10.1002/pat.3131.

(40) Brännström, S.; Malmström, E.; Johansson, M. Biobased UV-Curable Coatings Based on Itaconic Acid. *J. Coatings Technol. Res.* **2017**, *14* (4), 851–861. https://doi.org/10.1007/s11998-017-9949-y.

(41) Pezzana, L.; Mousa, M.; Malmström, E.; Johansson, M.; Sangermano, M. Bio-Based Monomers for UV-Curable Coatings: Allylation of Ferulic Acid and Investigation of Photocured Thiol-Ene Network. *Prog. Org. Coatings* **2021**, *150*, 105986. https://doi.org/https://doi.org/10.1016/j.porgcoat.2020.105986.

(42) Murayama, T.; Bell, J. P. Relation between the Network Structure and Dynamic Mechanical Properties of a Typical Amine-Cured Epoxy Polymer. *J. Polym. Sci. Part A-2 Polym. Phys.* **1970**, *8* (3), 437–445. https://doi.org/https://doi.org/10.1002/pol.1970.160080309.

(43) Shimbo, M.; Nishitani, N.; Takahama, T. Mechanical Properties of Acid-Cured Epoxide Resins with Different Network Structures. *J. Appl. Polym. Sci.* **1984**, *29* (5), 1709–1721. https://doi.org/https://doi.org/10.1002/app.1984.070290524.

(44) ASTM D3363-05. Standard Test Method for Film Hardness by Pencil Test. *ASTM Int.* **2005**. https://doi.org/10.1520/D3363-05.

(45) Mark, J. E.; Lee, C. Y. C.; Bianconi, P. A. Hybrid Organic-Inorganic Composites. *PA Bianconi, Eds* **1994**.

(46) Liu, F.; Liu, A.; Tao, W.; Yang, Y. Preparation of UV Curable Organic/Inorganic Hybrid Coatings-a Review. *Prog. Org. Coatings* **2020**, *145*, 105685. https://doi.org/https://doi.org/10.1016/j.porgcoat.2020.105685.

(47) Sangermano, M.; Amerio, E.; Epicoco, P.; Priola, A.; Rizza, G.; Malucelli, G. Preparation and Characterization of Hybrid Nanocomposite Coatings by Cationic UV-Curing and the Sol-Gel Process of a Vinyl Ether Based System. *Macromol. Mater. Eng.* **2007**, *292*, 634–640. https://doi.org/10.1002/mame.200600507.

(48) Amerio, E.; Malucelli, G.; Sangermano, M.; Priola, A. Nanostructured Hybrid Materials Obtained by UV Curing and Sol-Gel Processes Involving Alkoxysilane Groups: *e-Polymers* **2009**, *9* (1), 59. https://doi.org/doi:10.1515/epoly.2009.9.1.727.

(49) Sangermano, M.; Malucelli, G.; Amerio, E.; Priola, A.; Billi, E.; Rizza, G. Photopolymerization of Epoxy Coatings Containing Silica Nanoparticles. *Prog. Org. Coatings* **2005**, *54* (2), 134–138. https://doi.org/https://doi.org/10.1016/j.porgcoat.2005.05.004.

(50) Liang, B.; Chen, J.; Guo, X.; Yang, Z.; Yuan, T. Bio-Based Organic-Inorganic Hybrid UV-Curable Hydrophobic Coating Prepared from Epoxidized Vegetable Oils. *Ind. Crops Prod.* **2021**, *163*, 113331. https://doi.org/https://doi.org/10.1016/j.indcrop.2021.113331.

(51) Malucelli, G.; Priola, A.; Sangermano, M.; Amerio, E.; Zini, E.; Fabbri, E. Hybrid Nanocomposites Containing Silica and PEO Segments: Preparation through Dual-Curing Process and Characterization. *Polymer (Guildf).* **2005**, *46* (9), 2872–2879. https://doi.org/https://doi.org/10.1016/j.polymer.2005.02.045.

SYNOPSIS: This work exploits renewable furan building blocks and employs UV-radiation curing to form biobased epoxy thermosets and composites.

ABSTRACT GRAPHIC: